

Peripheral Neuropathies of the Median, Radial, and Ulnar Nerves: MR Imaging Features¹

CME FEATURE

See accompanying test at http://www.rsna.org/education/lrg_cme.html

LEARNING OBJECTIVES FOR TEST 1

After reading this article and taking the test, the reader will be able to:

- Describe basic MR imaging protocols for the evaluation of peripheral neuropathies.
- Identify and describe the normal anatomy in the region of the median, radial, and ulnar nerves.
- Recognize the MR imaging features of frequently occurring neuropathies of the median, radial, and ulnar nerves.

TEACHING POINTS

See last page

Gustav Andreisek, MD • David W. Crook, MD • Doris Burg, MD
Borut Marincek, MD • Dominik Weishaupt, MD

The median, radial, and ulnar nerves of the upper limbs may be affected by various peripheral neuropathies, each of which may be categorized according to its cause, as either an entrapment or a nonentrapment neuropathy. Entrapment neuropathies, also referred to as nerve compression syndromes, include the supracondylar process syndrome, pronator syndrome, anterior interosseous nerve syndrome, carpal tunnel syndrome, posterior interosseous nerve syndrome, cubital tunnel syndrome, and Guyon canal syndrome. Nonentrapment neuropathies include traumatic nerve injuries, infectious and inflammatory conditions, polyneuropathies, and mass lesions at anatomic locations where entrapment syndromes typically do not occur. Although clinical examination and electrophysiologic testing are the cornerstone of the diagnostic work-up, in certain cases magnetic resonance (MR) imaging may provide key information about the exact anatomic location of a lesion or may help narrow the differential diagnosis. In patients with a diagnosis of peripheral neuropathy, MR imaging may help establish the cause of the condition and provide information crucial for conservative management or surgical planning. In addition, knowledge of the normal anatomy and of the possible causes, typical clinical findings, and MR imaging features of peripheral neuropathies that affect the median, radial, and ulnar nerves allows greater confidence in the diagnosis.

©RSNA, 2006

Abbreviations: CIDP = chronic inflammatory demyelinating polyradiculoneuropathy, SE = spin echo, STIR = short inversion time inversion recovery

RadioGraphics 2006; 26:1267–1287 • Published online 10.1148/rg.265055712 • Content Codes: **MK** **MR**

¹From the Institute for Diagnostic Radiology, Department of Medical Radiology, University Hospital Zurich, Raemistrasse 100, CH-8091 Zurich, Switzerland (G.A., D.W.C., B.M., D.W.); and Division of Hand, Plastic and Reconstructive Surgery, Department of Surgery, University Hospital (Academic Medical Center), Zurich, Switzerland (D.B.). Received June 13, 2005; revision requested July 15 and received August 18; accepted August 26. All authors have no financial relationships to disclose. **Address correspondence to D.W.** (e-mail: dominik.weishaupt@usz.ch).

Introduction

For the evaluation of peripheral neuropathies, physicians traditionally relied primarily on information gained from an accurate clinical history, a thorough physical examination, and electrodiagnostic testing with electromyography, nerve conduction studies, and recordings of somatosensory evoked potentials (1,2). However, because such diagnostic tests and studies do not provide spatial information regarding the nerve and the surrounding structures, the information they provide is sometimes insufficient to establish the diagnosis (3). In equivocal cases, clinicians may ask for an additional imaging evaluation with either ultrasonography (US) or magnetic resonance (MR) imaging. The selection of the imaging modality to be used for further work-up for peripheral neuropathies depends on the anatomic location of the abnormality, the clinician's preference, local availability, and the individual experience of the radiologist with each modality.

MR imaging is considered useful for the assessment of neuromuscular disorders. It provides high-resolution depiction of nerves and allows visualization of primary abnormalities, such as a mass lesion compressing a nerve, as well as secondary abnormalities, such as nerve enlargement and enhancement due to neuritis (4). However, the primary nerve abnormality may not be visible in some cases. In such cases, the observation of signal intensity changes in the muscle that is innervated by the abnormal nerve may be used to diagnose and localize the nerve lesion (5).

Peripheral neuropathies may be categorized according to cause, as either entrapment or non-entrapment neuropathies. Entrapment neuropathies (also referred to as nerve compression syndromes) of the median, radial, and ulnar nerves are characterized by alterations of the nerve function that are caused by mechanical or dynamic compression. Nerve entrapment syndromes occur because of anatomic constraints at specific locations. Anatomic locations that are prone to nerve entrapment syndromes include sites where the nerve courses through fibro-osseous or fibromuscular tunnels or penetrates a muscle (6). If there is even a slight divergence from the normal anatomy or conditions at these locations—for example, an anatomic variant or a degenerative change—the passage may be narrowed, and nerve entrapment may result. In some cases, repetitive

stress from overuse may cause further narrowing of an already narrow passage and lead to nerve compression. Findings in patients with nonentrapment neuropathies may include traumatic nerve injuries, inflammatory conditions, polyneuropathies, and mass lesions at anatomic locations where entrapment does not typically occur.

This article surveys the anatomy and MR imaging appearances of the most common peripheral neuropathies of the upper extremity. We use the term *peripheral neuropathies of the upper extremity* to summarize abnormalities of the median, ulnar, and radial nerves. Since the three nerves arise from different cords of the brachial plexus, we discuss only nerve abnormalities that affect the nerves distal to the brachial plexus. Particular attention is given to the nerve compression syndromes that occur most frequently in the upper extremity.

Technical Considerations

Standard MR pulse sequences are used to visualize the anatomic features of normal and abnormal peripheral nerves and the tissues that surround them. In our experience, the axial plane is the most useful for assessment of peripheral nerves of the upper extremity, since all these nerves are longitudinally oriented within the limb. The use of T1-weighted spin-echo (SE) sequences allows depiction of fine anatomic detail, including the fascicular structure of the nerve. **A normal nerve on T1-weighted images appears as a smooth round or ovoid structure with an MR signal that is isointense to that in adjacent muscle. A rim of hyperintense signal often surrounds peripheral nerves. The T1-weighted sequence, when applied after the administration of an extracellular gadolinium-based contrast agent, can be useful for demonstrating the anatomic relationship of nerve fascicles to closely associated mass lesions (see the section "Mass Lesions" in this article).** Normal nerves do not appear enhanced after the intravenous administration of a gadolinium-based contrast agent. The MR signal in normal peripheral nerves on T2-weighted images acquired with fast SE or short inversion time inversion recovery (STIR) sequences is isointense to mildly hyperintense, compared with the signal intensity in normal muscle. Nerve fascicles may have a signal intensity slightly higher than that in the perineurium and internal perineural tissue.

The choice between conventional SE versus fast SE techniques is a matter of preference. At

Teaching
Point

our institution, STIR and T2-weighted fat-suppressed fast SE sequences are used, primarily because they require less acquisition time than do conventional SE sequences. STIR sequences offer the advantage of more-homogeneous fat suppression than can be achieved with T2-weighted fat-suppressed sequences, particularly in anatomic areas with irregular surfaces.

In patients in whom the presence of peripheral neuropathy is suspected, a thorough assessment of the signal characteristics of the muscles on T1-weighted SE and T2-weighted fat-suppressed or STIR images is of paramount importance. Since the nerve and the injury to it cannot always be visualized even with high-resolution MR imaging by using dedicated surface coils, the presence and the pattern of signal changes within muscles may be key in diagnosing nerve dysfunction. MR imaging can readily demonstrate abnormalities such as neurogenic muscle edema or fatty muscle atrophy. **STIR sequences are particularly sensitive in depicting muscle edema (5,7). Neurogenic muscle edema occurs in acute and subacute stages of denervation and results in prolongation of the T2 relaxation time at MR imaging with T2-weighted or STIR sequences as early as 24–48 hours after denervation.** In contrast, the signs of muscle denervation are not apparent at electromyography until 2–3 weeks after the onset of a nerve lesion (8,9). Muscle edema is caused by an enlargement of capillaries in the acute stage of lesion development, followed by the degeneration of fibers and the development of subsarcolemmal vacuoles in the subacute stage (8). In addition, direct neurogenic effects, secondary capillary changes owing to local vasodilators, local metabolic effects, and blood flow alterations are considered factors that may contribute to neurogenic muscle edema (8,10,11). Fatty muscle atrophy occurs when there is complete chronic muscle denervation. Fatty muscle atrophy evolves after several months of denervation and is most visible on standard T1-weighted SE images, which depict reduced volume and higher signal intensity compared with those of normal muscle tissue (12).

Entrapment Syndromes of the Median Nerve

The median nerve arises from the medial and lateral cords of the brachial plexus (C6 through C8, T1). The nerve follows the axillary artery and lies superficial to the brachial muscle in the upper arm. It enters the forearm between the two heads

of the pronator teres muscle. Just distal to that point, it gives off the anterior interosseous (antebrachial) nerve branch and then courses between the flexor digitorum superficialis and profundus muscles. Before passing under the flexor retinaculum and into the carpal tunnel, it gives off the superficial palmar branch. Distal to the carpal tunnel, it subdivides into digital and muscular branches. In the proximal part of the forearm (just distal to the elbow), the nerve innervates the pronator teres, flexor carpi radialis, palmaris longus, and flexor digitorum superficialis muscles. The anterior interosseous nerve supplies the flexor digitorum profundus, flexor pollicis longus, and pronator quadratus muscles. Muscles intrinsic to the hand that are innervated by the median nerve include the abductor pollicis brevis, the opponens pollicis, and the superficial head of the flexor pollicis brevis (5).

Neuropathies caused by entrapment of the median nerve include the supracondylar process syndrome, pronator syndrome, anterior interosseous nerve syndrome, and carpal tunnel syndrome.

Supracondylar Process Syndrome

Definition.—The supracondylar process syndrome is a very rare neuropathy that affects the median nerve at the level of the distal humerus. In patients with this condition, an osseous spur called the supracondylar process is visible on conventional radiographs at the anteromedial surface of the distal humerus. The supracondylar process may be connected to the medial epicondyle by a fibrous band, which is known as the ligament of Struthers (13).

Origins.—The supracondylar process is a congenital anatomic variation normally found in many amphibians, reptiles, and mammals but seldom found in humans. The ligament of Struthers is a remnant of a tendinous insertion of the latissimus dorsi muscle in the medial epicondyle, a structure typically found in climbing mammals (14).

Clinical Findings.—Patients experience paresthesia and numbness of the affected hand. Weakness and atrophy occur in some patients because of prolonged median nerve compression (14). Local pain is noticeable at physical palpation in those with a fracture of the supracondylar

process (15). Extension of the elbow may provoke symptoms such as paresthesia and numbness. In some patients, the supracondylar process is palpable at the distal aspect of the humerus. Discrepancies in muscle strength may be detected between the affected arm and the contralateral one. However, the presence of bilateral supracondylar process syndrome also should be considered (16). Electrodiagnostic studies may reveal signs of nerve compression, but the results of electrodiagnostic testing also may be normal in some cases (15). The differential diagnosis should include a high bifurcation of the brachial artery, a high origin of the pronator teres muscle, anomalous insertion of the coracobrachialis muscle, and other anatomic variants that could cause median nerve compression (6).

MR Imaging Features.—The MR imaging findings in patients with supracondylar process syndrome are not well described (14,15) but are probably unimportant, since the supracondylar process is well depicted on conventional radiographs. Apart from the supracondylar process, MR images may show the ligament of Struthers and its anatomic relationship to the median nerve (14). In addition, MR imaging may be useful for detecting a radiographically occult fracture of the supracondylar process (15).

Pronator Syndrome

Definition.—Pronator syndrome is characterized by chronic forearm pain due to entrapment or compression of the median nerve at the level of the pronator teres muscle.

Origins.—Pronator syndrome results from entrapment or compression of the median nerve between the humeral (superficial) and the ulnar (deep) heads of the pronator teres muscle, at the bicipital aponeurosis (lacertus fibrosus), or at the arch of the origin of the flexor digitorum superficialis (Fig 1). Compression and entrapment may result from anatomic constraints due to congenital abnormalities in the involved tendons or muscles, such as hypertrophy of the pronator teres muscle bellies or aponeurotic prolongation of the biceps brachii muscle (17). These conditions may be clinically silent for years and then suddenly become evident after repetitive pronation-supination stress (17). Less common causes of pronator syndrome include posttraumatic he-

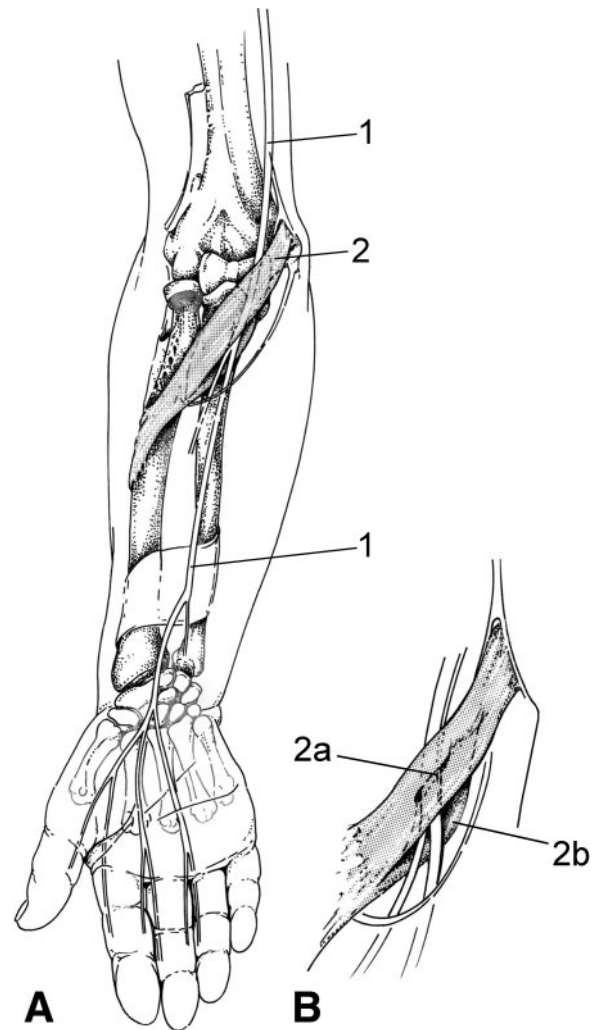
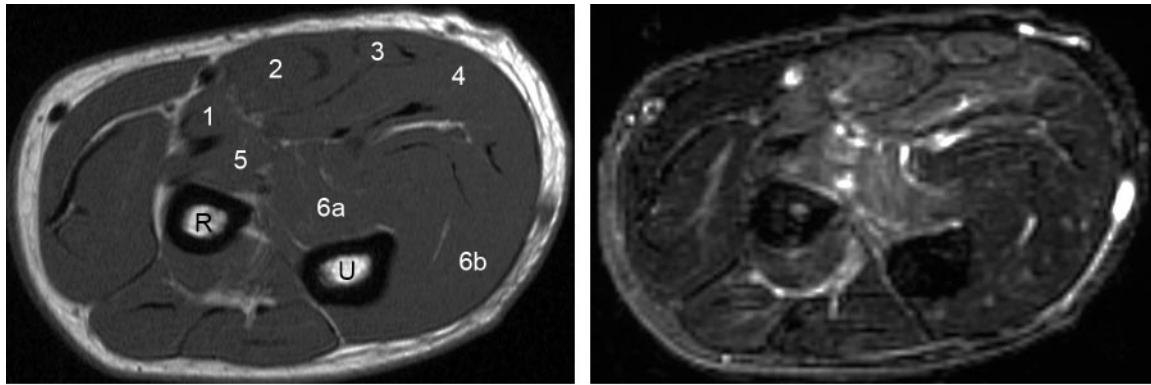


Figure 1. In *A*, the schematic provides an anterior view of the course of the median nerve (1) along the elbow, through the two heads of the pronator teres muscle (2), and into the forearm. *B* is a close-up detail of the most common site of pronator syndrome, where the nerve courses between the humeral head (2a) and the ulnar head (2b) of the muscle.

matoma, soft-tissue masses, prolonged external compression, and fracture of the elbow (eg, Volkmann fracture) (3).

Clinical Findings.—Patients with pronator syndrome experience pain and numbness in the volar aspect of the elbow and forearm as well as in the hand. Muscle weakness is not usually present. Physical examination produces pain at palpation of the pronator teres muscle, which may feel firm or have the appearance of a hard mass. A positive Tinel sign (dysesthesia produced by tapping over the nerve) may be present. The results of electrodiagnostic tests often are normal. Occasionally, denervation signs are observed in the pronator teres, flexor carpi radialis, and flexor digitorum



a. **Figure 2.** Pronator syndrome in a 58-year-old man after repeated pronation-supination stress from snow shoveling. **(a)** Axial T1-weighted SE MR image (repetition time msec/echo time msec, 560/9) at a middle level in the forearm shows normal volume and normal signal intensity of the proximal forearm muscles (1 = pronator teres, 2 = flexor carpi radialis, 3 = palmaris longus, 4 = flexor digitorum superficialis, 5 = flexor pollicis longus, 6a = radial part of the flexor digitorum profundus, 6b = ulnar part of the flexor digitorum profundus) and normal signal intensity of the radius (R) and ulna (U). **(b)** Corresponding T2-weighted fat-suppressed fast SE MR image (4340/106; echo train length, eight) demonstrates increased signal intensity indicative of edema in all of the muscles that are innervated by the median nerve. The ulnar part of the flexor digitorum profundus muscle, which is innervated by the ulnar nerve, is unaffected.

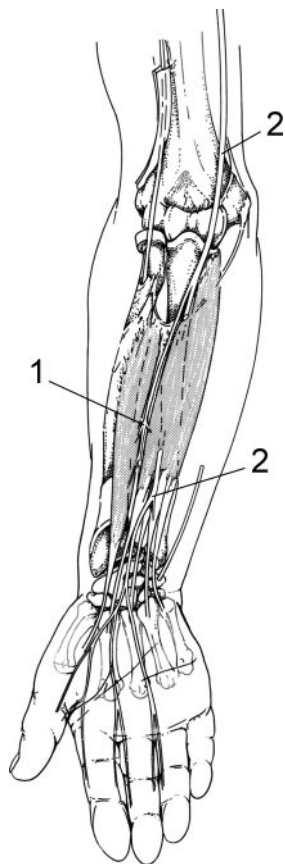


Figure 3. Schematic provides an anterior view of the course of the anterior interosseous nerve (1), which arises from the median nerve (2) in the forearm.

and overuse syndromes, particularly carpal tunnel syndrome (17,18).

MR Imaging Features.—The normal median nerve often is poorly depicted at the elbow because of the minimal amount of perifascial fat in this region (19). The median nerve usually is visible between the pronator teres and the brachialis muscles on axial images. It may appear normal at the site of entrapment. In some cases sequelae of nerve damage, such as thickening or signal abnormalities, are found. The anatomic basis of pronator syndrome is often inconspicuous at MR imaging unless there is a mass or an osseous fracture in proximity to the nerve. Therefore, when axonal degeneration occurs, a typical pattern of muscle denervation is key for the diagnosis of pronator syndrome. The pronator teres and other muscles innervated by the median nerve distally to the site of the lesion may show abnormally high signal intensity on T2-weighted fat-suppressed, STIR, or T1-weighted images (Fig 2).

Anterior Interosseous Nerve Syndrome

Definition.—Anterior interosseous nerve syndrome (also called Kiloh-Nevin syndrome) is caused by entrapment or compression of the anterior interosseous nerve in the proximal part of the forearm. Most lesions that lead to this syndrome have a location distal to that typical of lesions that cause pronator syndrome (Fig 3).

superficialis muscles at electromyography. Conduction velocity along the median nerve may be delayed at the antecubital fossa. The differential diagnosis should include cervical radiculopathy, brachial plexopathy, thoracic outlet syndrome,

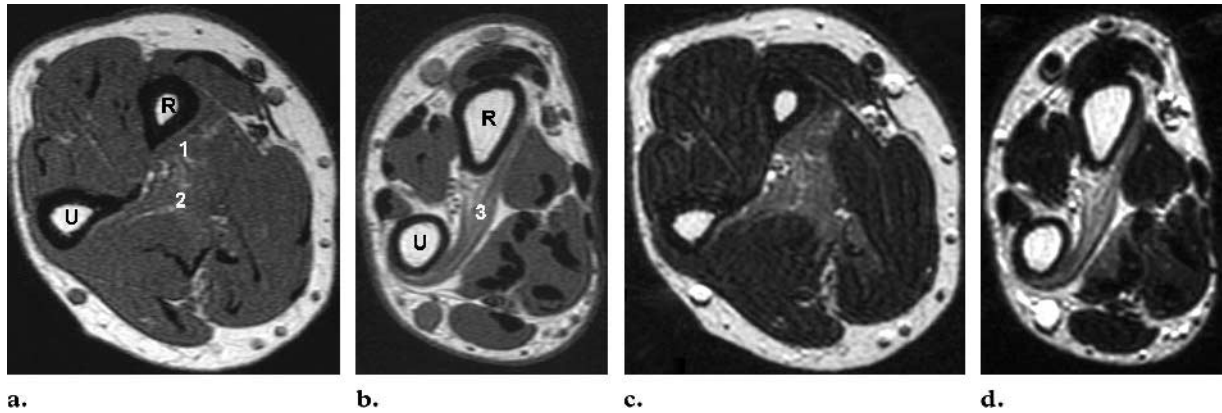


Figure 4. Complete anterior interosseous nerve syndrome in a 44-year-old man with weakness of the flexor muscles of the thumb and the second and third fingers. **(a, b)** Axial T1-weighted SE MR images (440/10) at proximal **(a)** and distal **(b)** levels of the forearm show moderate fatty atrophy in the flexor pollicis longus muscle (1 in **a**), in the radial aspect of the flexor digitorum profundus muscle (2 in **a**), and in the pronator quadratus muscle (3 in **b**). R = radius, U = ulna. **(c, d)** T2-weighted fast SE MR images (5160/98; echo train length, 10), at the same proximal **(c)** and distal **(d)** levels as **a** and **b**, depict increased signal intensity in the three muscles.

Origins.—The most frequent causes of anterior interosseous nerve syndrome are direct traumatic damage and external compression. Traumatic nerve damage may be the result of surgery, venous puncture, injection, or cast pressure. External compression of the anterior interosseous nerve may be caused by various anomalies, including a bulky tendinous origin of the ulnar (deep) head of the pronator teres muscle, a soft-tissue mass such as lipoma or ganglion, an accessory muscle, a fibrous band originating from the superficial flexor, or a vascular abnormality (6).

Clinical Findings.—Typically, patients with anterior interosseous nerve syndrome experience a dull pain in the volar aspect of the forearm, combined with an acute onset of muscle weakness. The muscle weakness affects the thumb, the index finger, and occasionally the middle finger because the deep flexor muscles of these fingers are innervated by the anterior interosseous nerve (6). Isolated weakness of the thumb, which occurs in some patients, may indicate isolated involvement of the particular fascicle that innervates the flexor pollicis longus (20). Since the anterior interosseous nerve does not innervate the skin, numbness is not associated with the syndrome.

Patients with anterior interosseous nerve syndrome are not able to form an “O” with the thumb and index finger. This characteristic find-

ing, called the circle sign, is due to a lack of innervation of the flexor pollicis longus muscle or the flexor digitorum profundus muscle (6). Muscle strength and forearm circumference may be decreased in the affected arm, compared with those in the unaffected arm (21). Electrodiagnostic studies may reveal denervation of the affected muscles (22). The differential diagnosis of anterior interosseous nerve syndrome includes isolated lesions of the flexor pollicis longus tendon, rheumatoid arthritis, fractures (humeral, radial, or ulnar), and a more proximal median nerve lesion in which the anterior interosseous nerve fibers are affected selectively or preferentially (so-called pseudo anterior interosseous nerve syndrome) (23,24). A mononeuritis such as Parsonage-Turner syndrome (neuralgic amyotrophy) may mimic anterior interosseous nerve syndrome clinically (25).

MR Imaging Features.—The anterior interosseous nerve usually is seen between the flexor digitorum superficialis and profundus muscles on MR images. In patients with typical anterior interosseous nerve syndrome with acute or subacute onset, axial T2-weighted fat-suppressed or STIR images depict increased signal intensity in the flexor digitorum profundus, flexor pollicis longus, and pronator quadratus muscles (Fig 4). Since the fourth and fifth fingers are not involved in anterior interosseous nerve syndrome, the MR signal intensity of the corresponding flexor muscles is normal (4). Most anatomic constraints and other entities that cause anterior

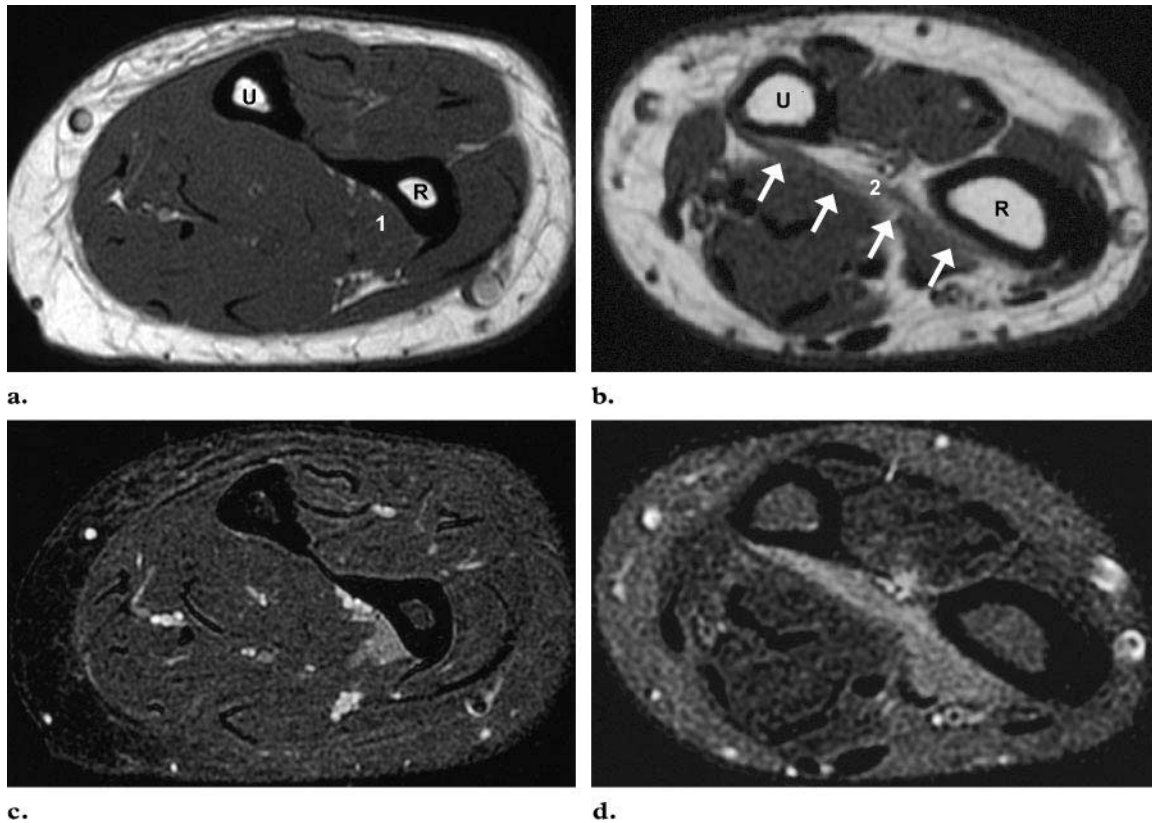


Figure 5. Incomplete anterior interosseous nerve syndrome in a 30-year-old woman with isolated weakness of the flexor pollicis longus and pronator quadratus muscles. (**a, b**) Axial T1-weighted SE MR images (340/15) obtained at proximal (**a**) and distal (**b**) levels in the forearm show a normal appearance of the flexor pollicis longus muscle (1 in **a**) and moderate fatty atrophy (arrows in **b**) of the pronator quadratus muscle (2 in **b**). R = radius, U = ulna. (**c, d**) Corresponding T2-weighted fat-suppressed fast SE MR images (3620/89; echo train length, 12), at the same proximal (**c**) and distal (**d**) levels as **a** and **b**, depict increased signal intensity in both muscles, a finding indicative of subacute denervation.

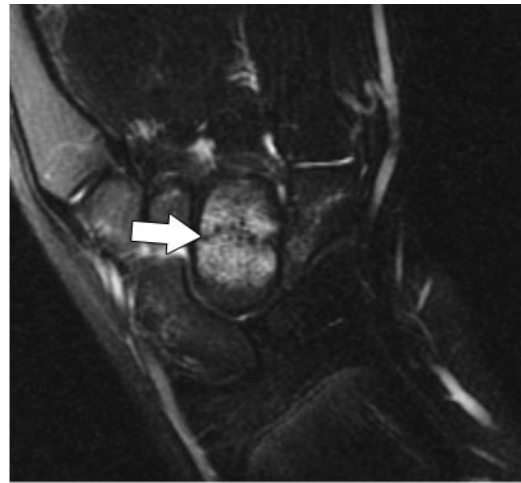
interosseous nerve syndrome are not visible at MR imaging (Fig 5). However, if focal entrapment or compression of the nerve is visible at MR imaging, this anatomic information may aid surgeons in avoiding long incisions that cross the antecubital fossa and may help minimize the invasiveness of the surgical procedure (6). Apart from its diagnostic utility, MR imaging is well suited for monitoring the effects of therapy in patients with anterior interosseous nerve syndrome, particularly the effects of conservative management with modification of activities, immobilization, anti-inflammatory medication, or physical therapy (21). Normalization of T2-weighted muscle signal intensity or of abnormalities on STIR images indicates the recovery of nerve function, whereas the additional development of T1-weighted MR signal intensity abnormalities indicates worsening and chronicity of anterior interosseous nerve syndrome (eg, with fatty muscle atrophy) (8).

Carpal Tunnel Syndrome

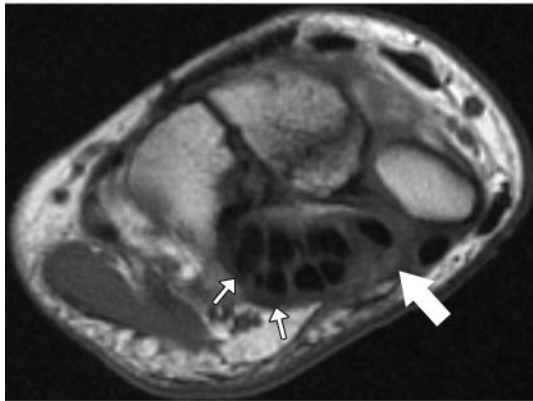
Definition.—Carpal tunnel syndrome is the most common peripheral neuropathy of the upper extremity and results from compression of the median nerve beneath the transverse carpal ligament. This syndrome most often affects middle-aged women.

Origins.—Carpal tunnel syndrome may result from any process that causes compression of the median nerve in the carpal tunnel (26). The potential causes of compression include various congenital, inflammatory, infectious, idiopathic, and metabolic or endocrine processes and conditions (eg, diabetes, pregnancy, and hypothyroidism) as well as trauma (Fig 6) and mass lesions (eg, ganglion, lipoma, neurofibroma, fibrolipomatous

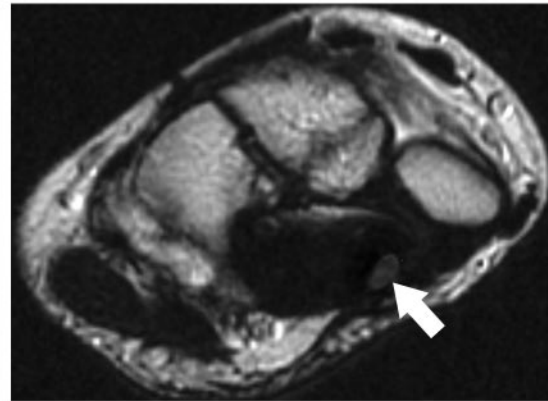
Figure 6. Carpal tunnel syndrome in a 14-year-old female patient with a wrist trauma-related fracture of the capitate bone. Electrodiagnostic testing revealed a complete conduction block of the median nerve at the level of the carpal tunnel. **(a)** Coronal T2-weighted fat-suppressed fast SE MR image (3500/100; echo train length, 12) of the wrist shows a fracture of the capitate bone (arrow) without dislocation. **(b)** Axial T1-weighted SE MR image (540/10) at the level of the carpal tunnel depicts moderate bowing of the flexor retinaculum (small arrows) and normal size of the median nerve (large arrow). **(c)** Axial T2-weighted fast SE MR image (4200/100; echo train length, 12) at the same level as **b** depicts increased signal intensity of the median nerve (arrow), a finding consistent with carpal tunnel syndrome.



a.



b.



c.

hamartoma) (Fig 7) (27). Repetitive use also may contribute to the development of carpal tunnel syndrome.

Clinical Findings.—Patients with carpal tunnel syndrome experience a burning wrist pain, which may radiate either proximally to the shoulder and neck region or distally into the fingers. An insidious onset of paresthesia or numbness in the thumb, index (second) finger, middle (third) finger, and the radial aspect of the fourth finger often is described; this pattern of numbness corresponds with the innervation pattern of the median nerve at the hand. Symptoms often are worse at night and are exacerbated by repetitive flexion and extension of the wrist, strenuous gripping, or exposure to vibration. In the later stages, patients experience clumsiness of the hand because of the thenar muscle weakness (1). A physical examination

with percussion may evoke tingling (the Tinel sign) in the median nerve at the wrist. Sensory nerve function may be abnormal and is easily evaluated by testing with a light touch or pinprick. Results of the Phalen maneuver (extreme flexion of the wrist to test for dysesthesia), Flick test (shaking of the hand to see whether symptoms are relieved), and percussion (for the Tinel sign) are frequently positive in patients with carpal tunnel syndrome. In severe or chronic cases, muscle atrophy of the thenar eminence may be present (28). Median nerve conduction testing may reveal a delayed conduction signal at the wrist, and needle-electrode electromyography may help detect denervation in the intrinsic hand muscles (22,27). The differential diagnosis in patients with carpal tunnel syndrome includes lesions of the central nervous system, cervical radiculopathy, brachial plexopathy, ulnar neuropathy at the elbow, and other focal neuropathies of the upper extremity, including proximal median nerve lesions (27).

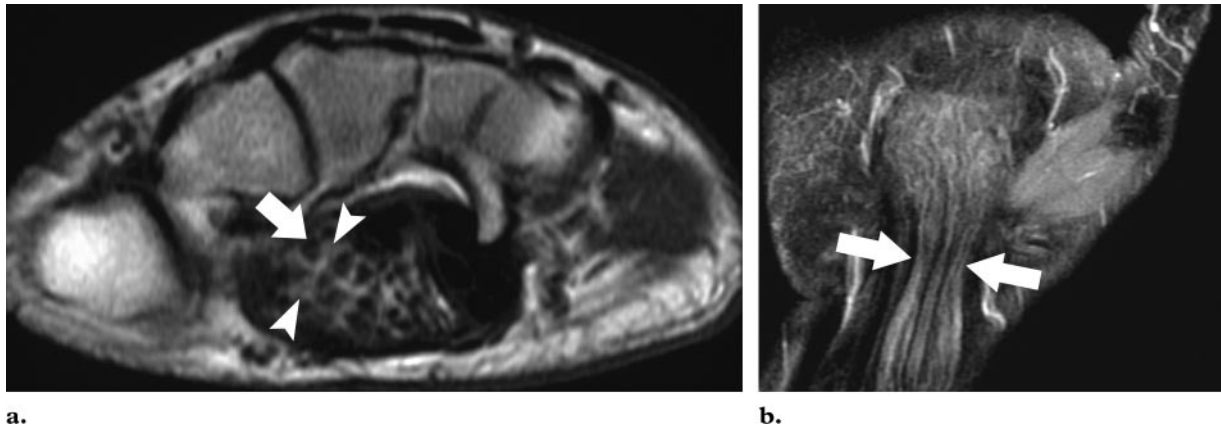


Figure 7. Carpal tunnel syndrome in a 54-year-old man with a fibrolipomatous hamartoma of the median nerve. **(a)** Axial T1-weighted SE MR image (380/10) at the level of the hook of the hamate shows enlargement of the median nerve, with hypointense nerve fascicles (arrow) surrounded by fibroadipose tissue (arrowheads). **(b)** Coronal contrast-enhanced T1-weighted fat-suppressed SE MR image (460/20) depicts entrapment of the median nerve within the carpal tunnel (arrows).

MR Imaging Features.—The median nerve usually is observed in a location superficial to the second flexor digitorum superficialis tendon or interposed between the flexor digitorum superficialis tendons and the flexor pollicis longus tendon (27). In axial cross-sectional views, the nerve usually appears ovoid in the proximal part of the carpal tunnel and has an increasingly flatter appearance at the level of the pisiform bone and in the distal part of the carpal tunnel. MR imaging findings in patients with carpal tunnel syndrome may be directly related to the nerve (size, shape, signal intensity) or to the other contents of the carpal tunnel. In carpal tunnel syndrome, nerve enlargement is best evaluated at the level of the pisiform bone, where its diameter is 1.6–3.5 times that at the level of the distal radioulnar joint (29,30). Flattening of the median nerve in patients with this syndrome is best evaluated by comparing the nerve diameter at the level of the hook of the hamate with that at the level of the distal radius (30). MR findings also may include increased nerve signal intensity on T2-weighted fat-suppressed or STIR images and bowing of the flexor retinaculum at the level of the hook of the hamate (27,30).

However, the sensitivity and specificity of all these MR signs for carpal tunnel syndrome are low (sensitivity, 23%–96%; specificity, 39%–87%), and for this reason MR imaging does not play a role in the clinical assessment of carpal tunnel syndrome (31). Nevertheless, MR imaging does have clinical utility when the cause of carpal tunnel syndrome is a neoplasm (eg,

neurofibroma), arthritis (eg, gouty tophi, rheumatoid tenosynovitis), or a congenital anomaly (eg, aberrant lumbrical muscles) and in evaluating the postoperative wrist.

Posterior Interosseous Nerve Syndrome and the Radial Nerve

Posterior interosseous nerve syndrome is a neuropathy caused by entrapment or compression of the radial nerve. The radial nerve arises from the posterior cord of the brachial plexus (C5 through C8, T1). The nerve follows the brachial artery dorsally, twists around the humerus, crosses under the teres major muscle, and then descends between the medial and lateral bellies of the triceps muscle, after which it courses through the spiral groove of the humerus. About 10 cm proximal to the lateral epicondyle, the radial nerve crosses from the dorsal aspect of the upper arm to the volar aspect of the elbow through the lateral intermuscular septum. Just anterior to the lateral epicondyle, the nerve subdivides into a deep motor branch and a superficial sensory branch. The deep motor branch penetrates the supinator muscle and courses downward along the dorsal aspect of the interosseous membrane. After it leaves the supinator muscle, the deep motor branch is referred to as the posterior interosseous nerve. The superficial sensory branch of the radial nerve follows the radial artery and innervates the

Teaching
Point

dorsal aspect of the thumb as well as the index finger and middle finger. At the level of the upper arm, the radial nerve gives off motor branches, which supply the triceps and anconeus muscles. At the level of the elbow, before entering the supinator muscle, the radial nerve gives off branches to supply the brachioradialis, extensor carpi radialis longus, extensor carpi radialis brevis, and supinator muscles. Distal to the latter, the most common branching pattern of the radial nerve is to the extensor digitorum, extensor carpi ulnaris, extensor digiti minimi, abductor pollicis longus, extensor pollicis brevis, extensor pollicis longus, and extensor indicis muscles (5,32).

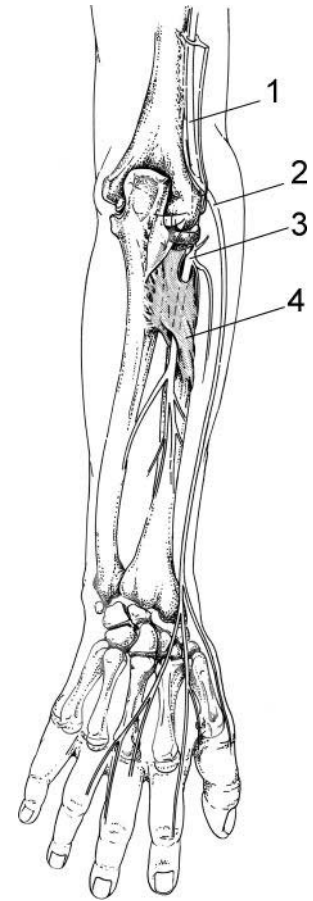
Definition

Posterior interosseous nerve syndrome, also referred to as deep radial nerve syndrome or supinator syndrome, results from radial nerve entrapment or compression at the level of the supinator muscle, in the proximal forearm (Fig 8). The syndrome may be manifested clinically in two different forms, with either pain or muscle weakness as the leading symptom (33).

Origins

There are various sites at which compression of the radial nerve may occur. The most common site of nerve compression is at the proximal edge of the supinator muscle. At this level, the arcade of Frohse may be found. The arcade of Frohse, a congenital variant that occurs in 30%–50% of the general population, is defined as a fibrous adhesion between the brachialis and brachioradialis muscles (32,34). Less common potential sites of radial nerve compression include fibrous adhesions and bands at the anterior radiohumeral joint capsule, abnormal recurrent blood vessels that cross the posterior interosseous nerve (leash of Henry), an intermuscular septum between the extensor carpi ulnaris and the extensor digitorum minimi muscle, and fibrous adhesions at the margin of the extensor carpi radialis brevis muscle and the distal margin of the supinator muscle (35). Posterior interosseous nerve syndrome occasionally is caused by overuse (eg, in athletes or in violinists), external compression (eg, due to use of crutches), radial head fracture, soft-tissue tumors (ganglion, lipoma), septic arthritis, synovial chondromatosis, or rheumatoid synovitis (34,36–42).

Figure 8. Schematic shows a posterior view of the course of the radial nerve through the elbow, forearm, and hand. The radial nerve (1) divides at the level of the elbow into the superficial radial nerve (2) and the posterior interosseous nerve (3). In posterior interosseous nerve syndrome, the most common site of radial nerve compression is where the nerve penetrates the supinator muscle (4).



Clinical Findings

Patients with posterior interosseous nerve syndrome present predominantly with forearm pain, a symptom that is nonspecific to posterior interosseous nerve syndrome. Other patients with posterior interosseous nerve syndrome describe weakness of the extensor muscles as the leading symptom. Since the superficial sensory branch of the median nerve branches off above the sites of compression in posterior interosseous nerve syndrome, no sensory disturbance or numbness is present. There is pain in the proximal forearm and tenderness in the nerve at the level of the supinator muscle (34). There is no Tinel sign. A typical hand position is seen in patients with posterior interosseous nerve syndrome: Since the extensor muscles of the fingers are affected, it is difficult or impossible to maintain finger extension. The fingers immediately droop in the palmar direction as soon as external extension is voluntarily ended. In addition, the hand deviates radially during wrist extension, because of weakness of the extensor carpi ulnaris muscle. Involuntary wrist flexion in the palmar direction, which is seen in complete radial nerve palsy, is not present in

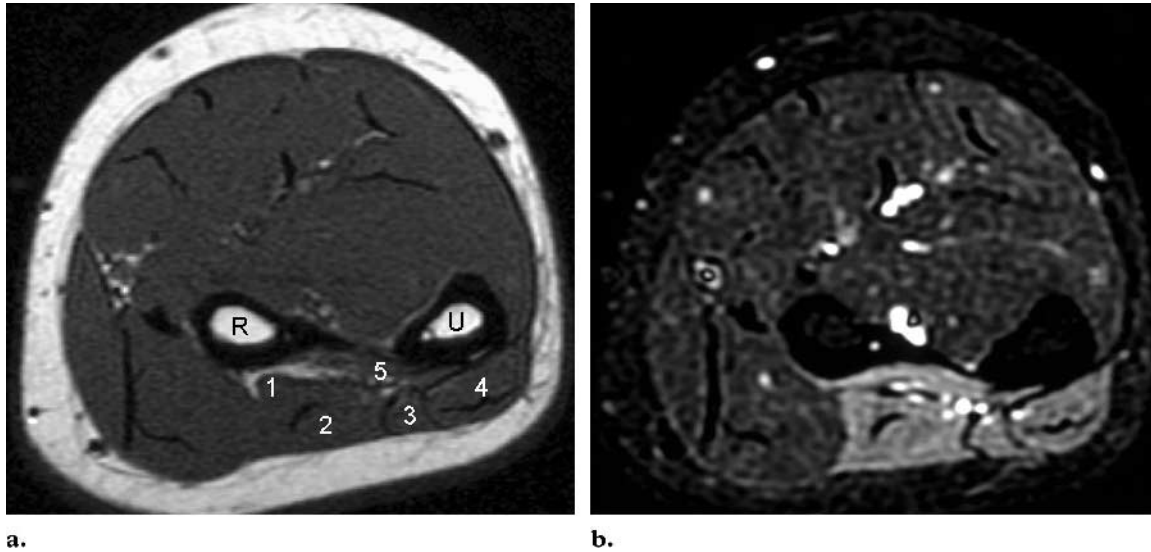


Figure 9. Posterior interosseous nerve syndrome in a 27-year-old woman with weakness of the extensor muscles of the hand. **(a)** Axial T1-weighted SE MR image (320/10) in the proximal part of the forearm shows a moderate loss of volume in the muscles (1 = abductor pollicis longus, 2 = extensor digitorum, 3 = extensor digiti minimi, 4 = extensor carpi ulnaris, 5 = extensor pollicis brevis and longus). R = radius, U = ulna. **(b)** Corresponding T2-weighted STIR MR image (repetition time msec/echo time msec/inversion time msec, 4840/54/150) depicts edema in the muscles, all of which are innervated by the posterior interosseous nerve.

patients with posterior interosseous nerve syndrome (6). Incomplete forms of posterior interosseous nerve syndrome occur in which only several fingers droop, depending on which muscles are affected (34). At electrodiagnostic studies, a conduction block or a prolongation of radial nerve conduction delays is seen at the site of compression. However, the results of electrodiagnostic testing in many patients may be normal or equivocal, and well-established electrophysiologic criteria for diagnosis do not yet exist (34). The differential diagnosis of posterior interosseous nerve syndrome commonly includes lateral epicondylitis, or tennis elbow, as well as other chronic pain syndromes of the forearm (43).

MR Imaging Features

In most people, the radial nerve can be detected easily on axial T1-weighted images as a low-signal-intensity structure at the elbow joint, where the nerve courses between the brachialis and brachioradialis muscles (3). The posterior interosseous nerve also may be identified more distally, where it penetrates the supinator muscle. As a result of compression, the posterior interosseous nerve may be depicted with high signal intensity on T2-weighted fat-suppressed or STIR images. In patients with posterior interosseous nerve syndrome, direct visualization of a compressive anatomic structure is seldom possible at MR imaging. Occasionally, the arcade of Frohse may be

seen as a low-signal-intensity band at the proximal edge of the supinator muscle (1). However, the diagnosis of posterior interosseous nerve syndrome is based primarily on the muscle denervation pattern, which may indicate the level of the nerve lesion. In general, a proximal lesion affects all muscles innervated by the radial nerve, whereas a more distally located lesion may spare muscles that are innervated by motor branches given off more proximally to the lesion (19). In a typical case of posterior interosseous nerve syndrome in which muscle weakness is the leading symptom, the supinator, extensor digitorum, extensor carpi ulnaris, extensor digiti minimi, abductor pollicis longus, extensor pollicis brevis, extensor pollicis longus, and extensor indicis muscles may have abnormal signal intensity, while the extensor carpi radialis muscle is spared (Fig 9). The exact site of the lesion in such cases may be determined even without direct visualization of the anatomic structure that compresses the posterior interosseous nerve. Controversy presently surrounds the question of what is the appropriate surgical therapy. However, in future, information gained with MR imaging may be of considerable value for surgical planning and management of posterior interosseous nerve syndrome (6).

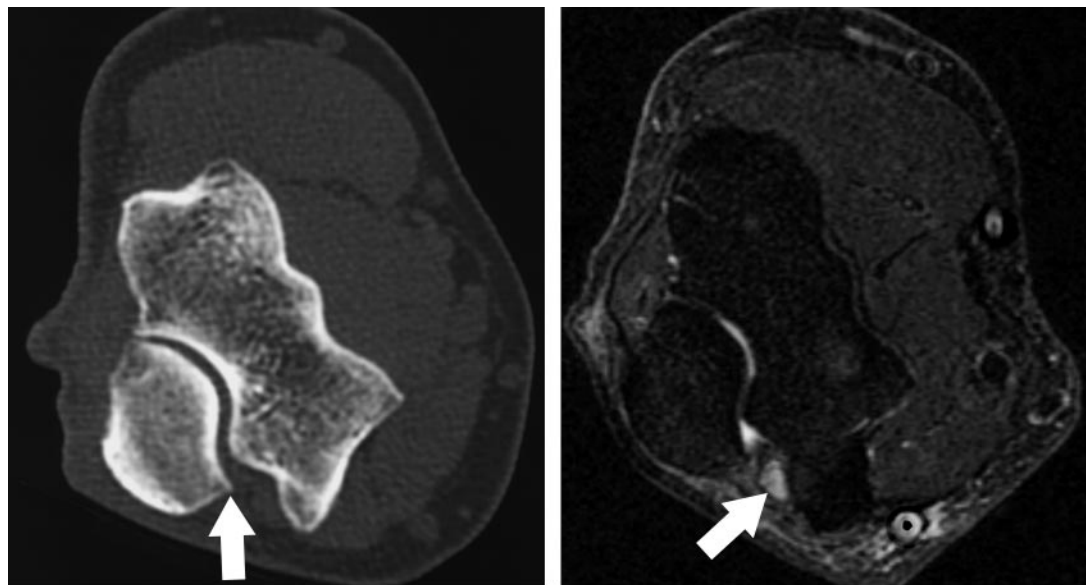


Figure 10. Ulnar neuritis in a 67-year-old man with numbness in the ulnar aspect of the palm and in the fingers. **(a)** Axial CT image shows an osteophyte in the medial aspect of the olecranon, at the level of the ulnar sulcus (arrow). **(b)** Corresponding axial T2-weighted STIR MR image (4200/54/150) depicts increased signal intensity in the ulnar nerve (arrow), a finding indicative of focal neuritis.

Entrapment Syndromes of the Ulnar Nerve

The ulnar nerve arises from the medial cord of the brachial plexus (C8 and T1). The nerve follows the brachial and axillary artery medially and downward to the midportion of the humerus. Subsequently, the nerve courses dorsally, penetrates the medial intermuscular septum, descends along the medial head of the triceps muscle, and finally enters the cubital tunnel, which is located at the medial condyle of the elbow. Distal to the cubital tunnel, the ulnar nerve lies between the two heads of the flexor carpi ulnaris muscle and courses distally between the flexor carpi ulnaris and the flexor digitorum profundus muscles to the volar aspect of the wrist (5). At the wrist, the ulnar nerve runs through the Guyon canal. Distal to the Guyon canal, it subdivides into superficial and deep motor branches. The deep motor branch first courses laterally to the hypothenar muscles and then proceeds medially, deep to the intrinsic muscles of the hand. At the level of the upper arm, there are no muscles innervated by the ulnar nerve. At the level of the elbow, the ulnar nerve gives off motor branches to the flexor carpi ulnaris and to the ulnar half of the flexor digitorum profundus muscle. The radial half of the latter is innervated by the anterior interosseous nerve (see “Entrapment Syndromes of

the Median Nerve”). In the distal part of the forearm, the ulnar nerve gives off a dorsal sensory branch that innervates the ulnar aspect of the dorsum of the hand. In the palm, the superficial branch innervates the palmaris brevis muscle, the skin of the ulnar aspect of the palm, and the ulnar side of the fourth and fifth fingers. The deep motor branch supplies the hypothenar muscles (ie, abductor digiti minimi, flexor digiti minimi, and opponens digiti minimi), the deep head of the flexor pollicis brevis, the adductor pollicis, and the dorsal and palmar interosseous muscles, as well as the third and fourth lumbrical muscles of the hand (44).

The neuropathies produced by entrapment of the ulnar nerve include cubital tunnel syndrome and Guyon canal syndrome.

Teaching Point

Cubital Tunnel Syndrome

Definition.—Cubital tunnel syndrome is the second most common peripheral neuropathy of the upper extremity. Moderate compression of the nerve within the cubital tunnel, such as occurs due to physiologic decrease in cubital tunnel volume during elbow flexion, may be normal and may not result in neuropathy (45). Cubital tunnel syndrome arises from pathologic compression or a lesion of the ulnar nerve within the cubital tunnel, where the nerve passes beneath the cubital tunnel retinaculum (also known as the epicondyl-olecranon ligament or Osborne band) (6).

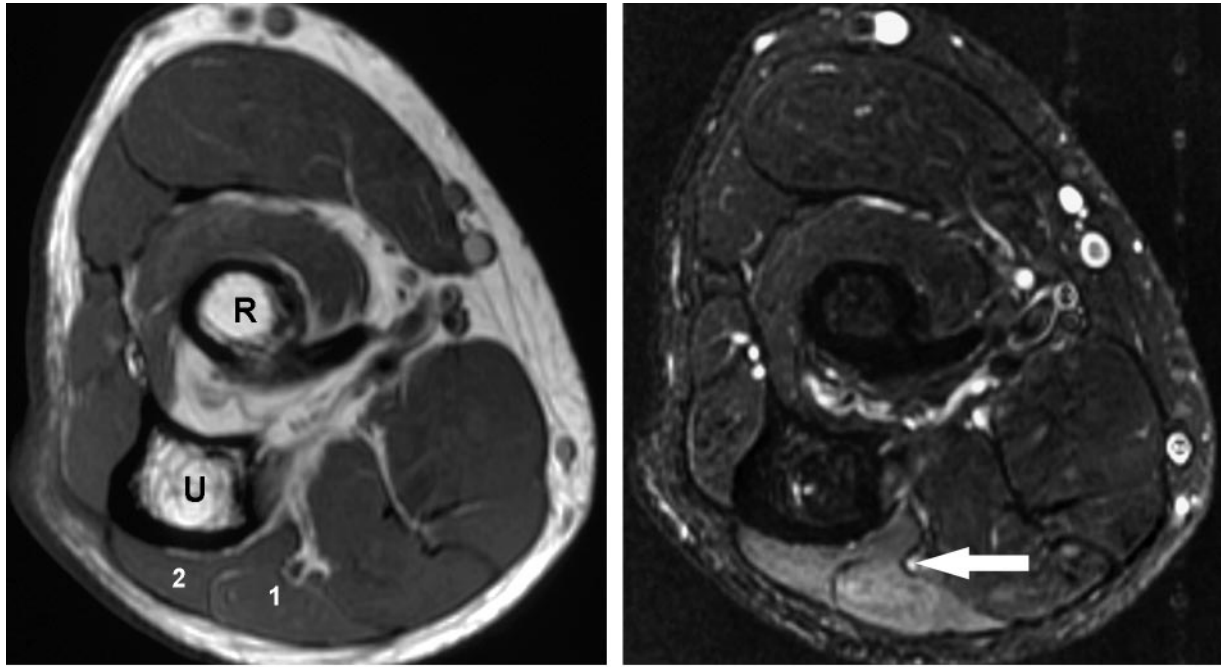


Figure 11. Cubital tunnel syndrome in a 44-year-old man with pain in the forearm while playing the transverse flute. Axial T1-weighted SE MR image (500/16) (**a**) and corresponding axial T2-weighted fat-suppressed SE MR image (5340/58) (**b**) depict normal muscle volume but high signal intensity in the flexor carpi ulnaris (1 in **a**) and flexor digitorum profundus (2 in **a**) muscles, respectively. Increased signal intensity in the ulnar nerve in **b** is indicative of focal neuritis (arrow). *R* = radius, *U* = ulna.

Origins.—The possible causes of cubital tunnel syndrome include overuse, subluxation of the ulnar nerve because of congenital laxity in the fibrous tissue, humeral fracture with loose bodies or callus formation, an arthritic spur arising from the epicondyle or olecranon, a muscle anomaly (eg, an anconeus epitrochlearis muscle), a soft-tissue mass, ganglion, osteochondroma, synovitis secondary to rheumatoid arthritis, infection (eg, tuberculosis), and hemorrhage. Other possible causes include acute or chronic external compression (eg, “sleepy palsy,” perioperative damage), trauma (eg, from use of a jackhammer), and compression by a thickened retinaculum (or arcuate ligament) of the flexor carpi ulnaris muscle (6,46,47).

Clinical Findings.—Patients typically experience pain in the medial aspect of the elbow, and the pain usually worsens with elbow flexion. In addition, patients may have paresthesia or numbness in the ulnar aspect of the palm and in the fingers. Many also experience weakness that affects all the muscles that are innervated by the ulnar nerve. Physical examination reveals tenderness over the cubital tunnel. The ulnar nerve may undergo subluxation during palpation at the medial epicondyle. Typically, a clawlike position of the hand is seen in patients with ulnar nerve le-

sions. Cutaneous sensation is impaired in the ulnar sensory area. The results of electrodiagnostic testing may indicate either a decrease in nerve conduction velocity or a complete failure of nerve conduction at the elbow. Discriminative testing of the ulnar nerve may help determine the precise location of the lesion (2).

MR Imaging Features.—Within the cubital tunnel, the normal ulnar nerve is most visible posterior to the medial epicondyle on axial T1-weighted MR images, on which it appears as a round hypointense structure surrounded by fat. In patients with cubital tunnel syndrome, the nerve may appear with increased signal intensity on images acquired with T2-weighted or STIR sequences (Fig 10). Ulnar nerve dislocation is perhaps most clearly seen on axial images acquired during elbow flexion (3). In the presence of nerve entrapment, MR images may depict osteoarthritis, synovitis, bone and muscle anomalies, or masses as the cause of the syndrome. MR imaging findings indicative of ulnar muscle denervation include edema or fatty atrophy of the flexor digitorum profundus, flexor carpi ulnaris (Fig 11), and any of the ulnar intrinsic muscles of the

hand. MR images of the elbow region often are obtained to substantiate the clinical diagnosis or determine the cause of cubital tunnel syndrome or of failed ulnar nerve transposition surgery (6). In addition, MR imaging of the cervical spine, the brachial plexus, the thoracic outlet, and the upper arm and forearm (including the wrist and hand) may be performed to rule out the so-called double-crush phenomenon in some patients. In the presence of the double-crush phenomenon, compression at one point along a nerve causes an increased susceptibility to compression neuropathy along the entire course of the nerve (34).

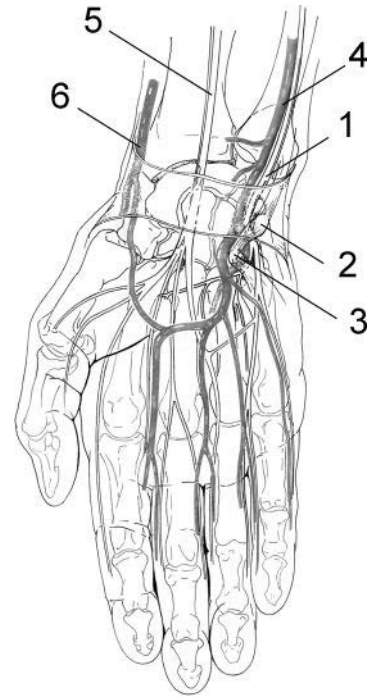
Guyon Canal Syndrome

Definition.—Guyon canal syndrome results from a lesion of the ulnar nerve at the level of the Guyon canal (also called the pisohamate tunnel) (Fig 12). The roof of the Guyon canal consists of the palmar carpal ligament, the palmaris brevis muscle, and the origins of the hypothenar muscles. The tendons of the flexor digitorum profundus, the transverse carpal ligament, the pisohamate and pisometacarpal ligaments, and the opponens digiti minimi form the floor of the Guyon canal. The medial border includes the pisiform bone and the flexor carpi ulnaris tendon. The lateral wall consists of the tendons of the extrinsic flexors, the transverse carpal ligament, and the hook of the hamate. The Guyon canal begins at the proximal edge of the volar carpal ligaments and ends at the fibrous arch of the hypothenar muscles (48,49).

Origins.—Possible causes of ulnar nerve lesions at the Guyon canal include ganglia, lipomas, and other cysts; anomalies of ligaments or muscles; ulnar artery aneurysms; fractures of the radius, pisiform bone, hook of the hamate, or other wrist bones; and chronic repetitive trauma, as in handlebar palsy in cyclists (44,50–58).

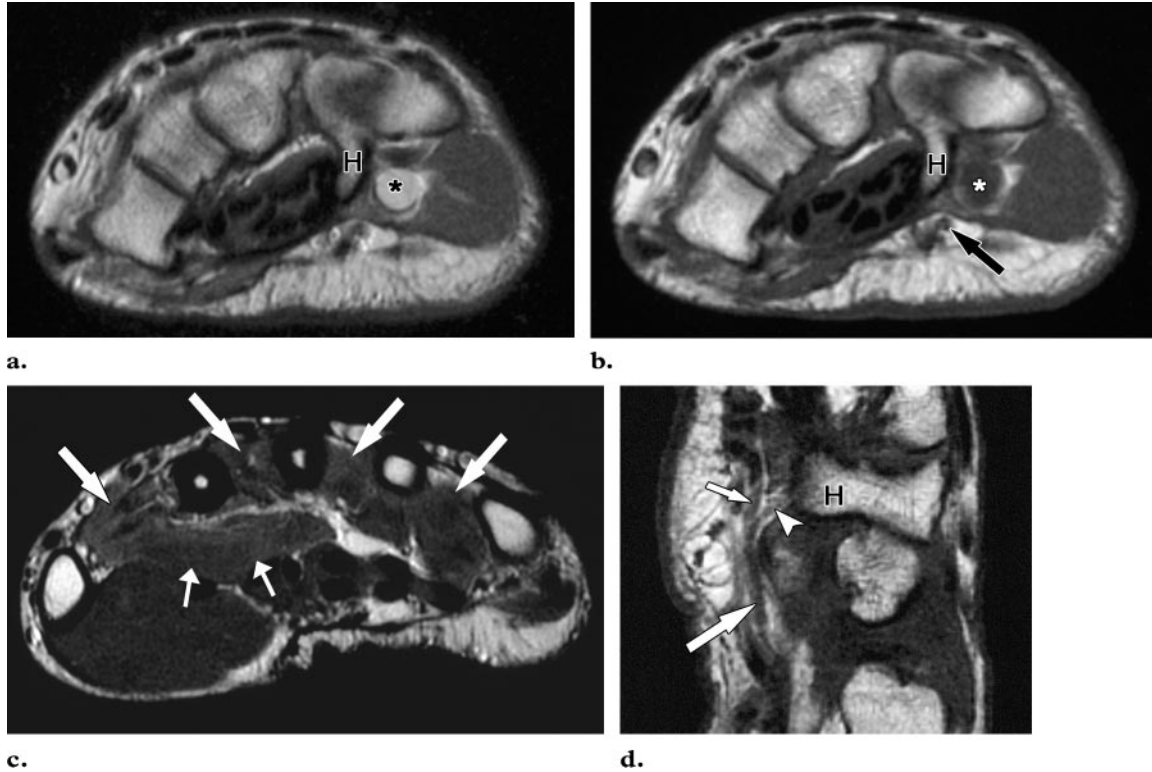
Clinical Findings.—Patients experience wrist pain, sensory abnormalities, and muscle weakness that affects the fingers. In Guyon canal syndrome, symptoms depend on the site of the lesion in regard to the ulnar nerve bifurcation. The most common lesion (type 1 lesion) is found in a site proximal to the Guyon canal and is characterized by sensory loss combined with weakness of all ulnar intrinsic hand muscles. An isolated lesion of the deep motor branch in a location immediately distal to the bifurcation (type 2 lesion) affects all ulnar intrinsic hand muscles but produces no sen-

Figure 12. Schematic provides a palmar view of the course of the ulnar nerve (1) as it passes through the Guyon canal, which is located between the pisiform bone (2) and the hook of the hamate (3). In addition to the ulnar nerve, the Guyon canal contains the ulnar artery (4), fat, and, occasionally, veins. 5 = median nerve, 6 = radial artery.



sory loss. A lesion of the deep motor branch in a location distal to the hypothenar branches (type 3 lesion) affects the interosseous and lumbrical muscles but spares the hypothenar muscles. Sensory loss without weakness is indicative of an isolated lesion of the superficial branch (type 4 lesion) (44,46). Physical examination typically reveals tenderness during percussion over the ulnar nerve at the wrist, particularly in patients in whom sensory fibers of the ulnar nerve are affected. The result of two-point discrimination and sensation tests may be abnormal at the ulnar aspect of the fourth and fifth fingers. The result of sensory testing at the dorsum of the hand is normal, since this area is innervated by the dorsal branch of the ulnar nerve. Weakness or atrophy of intrinsic hand muscles also may be present, depending on the site of the lesion and the corresponding muscle denervation pattern. Decreased strength during pinching and gripping, and an abduction deformity of the small finger (also known as Wartenberg sign of the ulnar nerve), also may be observed. The results of electrodiagnostic testing reveal prolonged distal motor latency or conduction failure along the ulnar fibers to the hypothenar muscles or the first dorsal interosseous muscle, combined with a normal sensory response of the dorsal ulnar nerve (2). The differential diagnosis includes abnormalities of the ulnar artery, more proximal ulnar neuropathies (eg, cubital tunnel syndrome, thoracic outlet syndrome, cervical radiculopathy), amyotrophic lateral sclerosis, focal motor neuron myelopathy, syringomyelia, and Pancoast tumor (6,59).

Figure 13. Ulnar nerve compression due to a ganglion cyst in the hand of a 57-year-old man. **(a)** Axial intermediate-weighted MR image (3500/40) at the level of the hook of the hamate (*H*) shows a hyperintense ganglion cyst (*). **(b)** Corresponding axial T1-weighted SE MR image (420/11) demonstrates the location of the ganglion cyst (*) next to the hook of the hamate (*H*) and near the ulnar nerve (arrow). **(c)** Axial intermediate-weighted MR image (3500/40) at the level of the metacarpal bones shows increased signal intensity in the adductor pollicis (small arrows) and in all the interosseous muscles (large arrows). **(d)** Sagittal T1-weighted SE MR image (540/12) at the level of the hook of the hamate (*H*) depicts the ulnar nerve (large arrow) and its bifurcation into a superficial sensory branch (small arrow) and a deep motor branch (arrowhead).



MR Imaging Features.—T1-weighted sequences are best suited for identifying the ulnar nerve within the Guyon canal. On T1-weighted images, the nerve appears as a round or ovoid structure surrounded by a small amount of fat. The bifurcation of the ulnar nerve normally is well depicted, and the course of both branches can be followed distally (3). In patients with ulnar nerve lesions in the Guyon canal, the size and signal intensity of the nerve should be assessed. MR imaging may help exclude the presence of a mass lesion and may demonstrate compression by an anomalous or accessory muscle or fibrous band (3). Furthermore, MR imaging is an excellent method for detecting abnormalities in the intrinsic hand muscles (Fig 13). The pattern of muscle abnormalities seen at MR imaging correlates well with the pattern of clinical findings of muscle denervation.

Nonentrapment Neuropathies

Apart from the anatomically defined locations in which compression neuropathies (entrapment syndromes) occur, peripheral neuropathies may occur at any site along the course of the median,

ulnar, and radial nerves. Nonentrapment neuropathies are peripheral neuropathies that are not caused by nerve impingement at predisposed anatomic locations. Nonentrapment neuropathies include neuropathies due to nerve injuries and infections, inflammatory demyelinating polyradiculoneuropathies, and polyneuropathies and neuropathies caused by masses.

Nerve Injuries

Most patients with an acute peripheral nerve injury are not referred for MR imaging. Patients in whom acute nerve transection is diagnosed on the basis of clinical history combined with the results of physical and electrodiagnostic examinations usually undergo surgery. However, many injuries do not result in transection of the nerve (1). In patients without nerve transection, it may be difficult for clinicians to distinguish between nerve lesions that recover on their own (neurapraxic and axonotmetic lesions, according to the Seddon classification system) and nerve lesions that do not recover spontaneously and may require surgery (neurotmetic lesions). MR imaging can aid

differentiation between axonometric and neurotmetic lesions on the basis of nerve and muscle signal intensity characteristics at different time intervals after nerve injury (57). In axonometric lesions, with axonal regeneration over time, there is a complete remission of any abnormality of either the nerve or the innervated muscle. The length of time needed for axonal regeneration may vary, depending on the severity of the nerve lesion. In contrast, MR abnormalities in neurotmetic lesions do not resolve over time, because the nerve does not regenerate (8,11). A typical electrodiagnostic finding in neurapraxic nerve lesions is focal blockage or slowing of nerve conduction. Motor unit action potentials may be normal. Typical MR imaging findings in neurapraxic nerve lesions are a focal increase in nerve signal intensity on T2-weighted and STIR images, combined with moderate or no abnormalities in muscle signal intensity. In axonometric nerve lesions, a deficit of nerve conduction distal to the injury is observed initially at electrodiagnostic testing and gradually reaches its peak after 1–2 weeks. Axonometric lesions recover within several weeks after axonal regeneration. Typical MR imaging findings in axonometric lesions include transient increases in nerve signal intensity distal to the site of injury on T2-weighted and STIR images, followed by normalization of the nerve signal intensity with axonal regeneration. In addition, transient signs of muscle denervation may appear as early as 24–48 hours after injury, findings that normalize gradually with muscle reinnervation. At electrodiagnostic testing, axonal degeneration in neurotmetic lesions typically is manifested as a persistent absence of nerve conduction distal to the injury. At MR imaging, increased nerve signal intensity on T2-weighted and STIR images disappears very late, and transient muscle denervation signs (eg, neurogenic edema) typically are followed by muscle volume reduction and fatty atrophy of muscle (1).

The increased signal intensity seen in injured peripheral nerves on T2-weighted and STIR images may reflect endoneurial or perineurial edema as a result of changes in the blood-nerve barrier; changes in water content due to altered axoplasmic flow; inflammation, as evidenced by a macrophage response; or the presence of axonal and myelin breakdown products (60,61). MR imaging of acute nerve injuries and nerve recovery may advance in future through the use of new MR imaging techniques and contrast agents (eg, small

superparamagnetic iron oxide particles) that may enable the depiction of macrophage activity in injured nerves (61). Together these techniques may aid clinicians in deciding between surgery and conservative management.

Infections

Various viral and bacterial infectious agents may cause a neuropathy in which the clinical symptoms mimic those of a focal nerve disturbance. The most common infectious agents include human immunodeficiency virus, varicella-zoster virus, herpes simplex virus, poliomyelitis virus, and cytomegalovirus. Bacterial infections such as leprosy, tuberculosis, and diphtheria also may lead to neuropathic manifestations. Clinical history, physical examination, and laboratory testing are the keys to diagnosis. MR imaging has no utility for evaluating peripheral nerves in patients with infectious neuropathies.

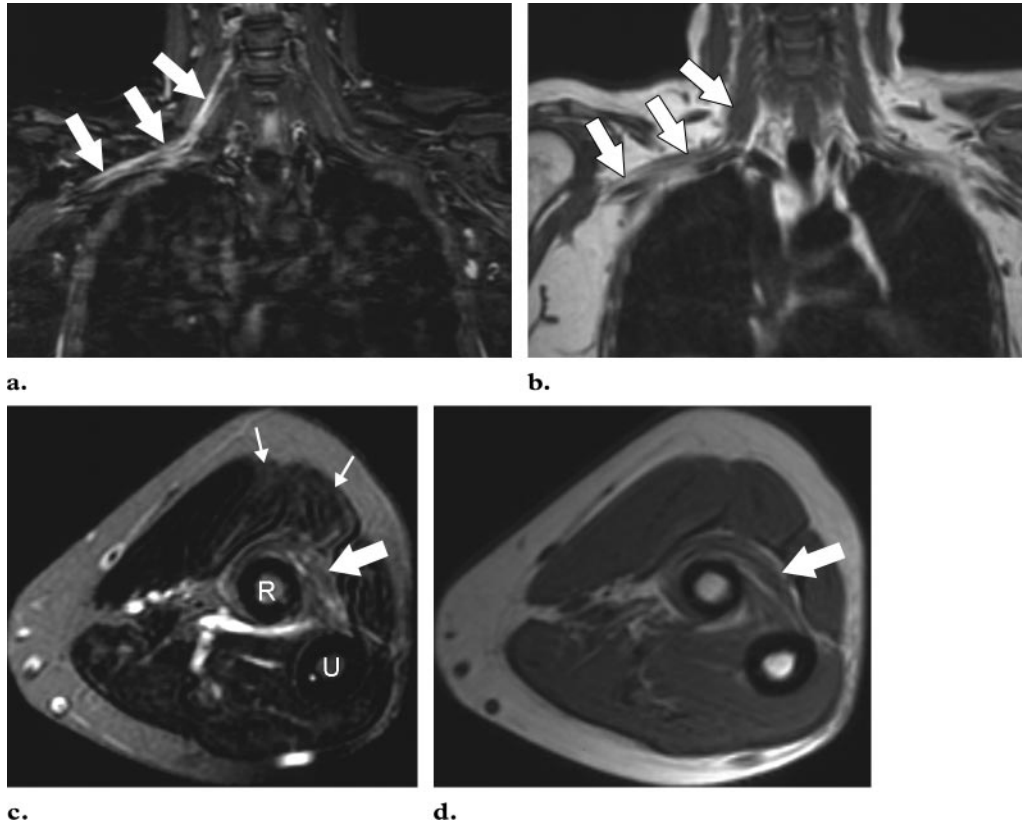
Inflammatory Demyelinating Polyradiculoneuropathies

Inflammatory demyelinating polyradiculoneuropathies are immune-mediated neuropathies characterized by multiple foci of demyelination and axonal degeneration of peripheral nerves. The classification of inflammatory demyelinating neuropathies is based on whether their onset is acute or chronic.

The most common acute inflammatory demyelinating polyradiculoneuropathy is Guillain-Barré syndrome, which is manifested with rapidly progressive muscle weakness and hyporeflexia. The legs are usually affected first, with subsequent ascending involvement of the arms and the face. In patients with Guillain-Barré syndrome, MR imaging of the spine and cauda equina may show nerve root enhancement or mild enhancement of intrathecal nerve roots after the administration of a gadolinium compound. This enhancement corresponds to the characteristic perineurial inflammatory and demyelinating processes of Guillain-Barré syndrome (62).

Several forms of chronic inflammatory demyelinating polyradiculoneuropathy (CIDP) have been described. They are named, according to the associated clinical manifestations and symptoms, as follows: classic CIDP, sensory CIDP, multifocal acquired demyelinating sensory and motor neuropathy, distal acquired demyelinating sensory neuropathy, and multifocal motor neuropathy with or without conduction block (63). These conditions differ not only in their clinical manifestations but also in their electrophysiologic and

Figure 14. Multifocal motor neuropathy in a 45-year-old female patient with nonspecific muscle weakness of the right arm. (**a, b**) Coronal fat-suppressed STIR image (5300/32/150) (**a**) and corresponding T1-weighted SE image (440/8) (**b**) show increased signal intensity and thickening, respectively, of the right brachial plexus (arrows). (**c, d**) Axial T2-weighted fast SE image (4000/100; echo train length, 12) (**c**) and corresponding T1-weighted SE image (620/9) (**d**) depict edema and atrophy of the supinator muscle (large arrow). Parts of the extensor muscles (small arrows in **c**) also are involved. *R* = radius, *U* = ulna.



laboratory features and their responses to treatment. However, the classification system is still being developed as advanced laboratory analyses lead to a better understanding of these complex neurologic disorders (64). To date, only a few subtypes of CIDP have been investigated with MR imaging. This section provides a brief overview of the MR imaging characteristics of classic CIDP, multifocal motor neuropathy, and CIDP coincident with monoclonal gammopathy.

MR imaging characteristics of classic CIDP are similar to those of multifocal motor neuropathy. Classic CIDP is characterized by a progressive symmetric weakness of the limbs, whereas multifocal motor neuropathy has an asymmetric distribution (Fig 14). Increased signal intensity of the affected nerves may be observed on T2-weighted or STIR images (a finding that may be associated with diffuse nerve swelling), and contrast enhancement of the nerves may be observed on T1-weighted images after the intravenous administra-

tion of a gadolinium chelate (65). The pathologic substrate of these MR imaging findings is not known; however, signal intensity abnormalities may result from demyelination or increased permeability of the blood-nerve barrier, while nerve swelling may be caused by inflammation and edema (65). In classic CIDP, onion bulb-type hypertrophic changes due to repetitive demyelination and remyelination also may be observed along the course of the median, radial, and ulnar nerves on MR images (66).

CIDP also may occur in association with monoclonal gammopathy of unknown significance. It may be difficult on the basis of clinical findings in some patients to distinguish between CIDP associated with monoclonal gammopathy of unknown significance and a distal demyelinating peripheral neuropathy. In these patients, MR

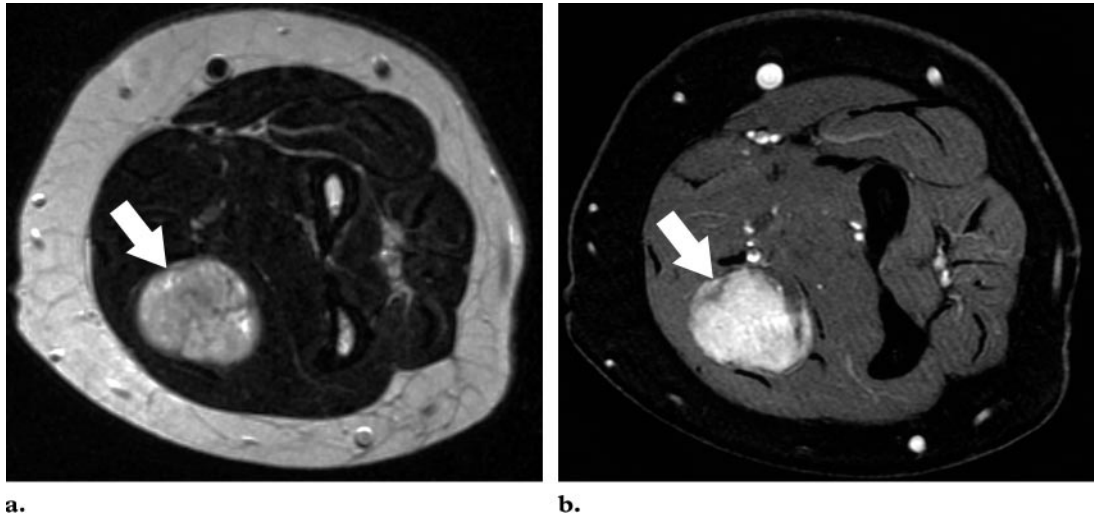


Figure 15. Schwannoma of the ulnar nerve in a 59-year-old woman. Axial T2-weighted fast SE MR image (4060/90) (**a**) and corresponding contrast-enhanced T1-weighted fat-suppressed fast spoiled gradient-recalled-echo MR image (205/3) (**b**) demonstrate a fusiform mass (arrow) at the location of the ulnar nerve in the forearm.

images may depict the proximal distribution pattern of the nerve abnormalities, which is characteristic of CIDP associated with monoclonal gammopathy and is not seen in distal demyelinating peripheral neuropathies (64). Typical findings at MR imaging of the spine, brachial plexus, and proximal median, radial, and ulnar nerves include increased signal intensities on T2-weighted or STIR images and swelling of the nerve roots, brachial cord, and proximal nerves. Contrast enhancement of the nerves usually is not seen (64).

Polyneuropathies

Polyneuropathies are differentiated on the basis of the location of the lesion, which may affect the perikaryon of the nerve cells (in the presence of a high concentration of mercury, aluminum, or cadmium, or with medications such as adriamycin and vincristine); the axon (in patients with diabetes mellitus, ethanol intoxication, uremia, or a deficiency of thiamin or pyridoxine); the nerve sheath (in patients with sphingolipidosis, paraproteinemia, or a hereditary neuropathy such as Charcot-Marie-Tooth disease); and the soft tissue that surrounds the peripheral nerves (in patients with vasculitis or a metabolic disease). In patients with a polyneuropathy, MR imaging of the brain or the spine may reveal involvement of the central

nervous system. MR imaging of the peripheral nerves is not well established. However, MR imaging of the arm may show muscle abnormalities associated with axonal neuropathies. Typical MR imaging findings are increased muscle signal intensity on T1-weighted images (a result of fatty muscle degeneration due to chronic denervation) and on T2-weighted images (a result of acute or subacute muscle degeneration) (67).

Mass Lesions

Mass lesions of peripheral nerves may be classified as lesions that originate from nerve or nerve sheath cells (ie, benign and malignant neurogenic tumors) or as lesions that originate from surrounding soft tissues. Benign neurogenic tumors include schwannomas (also called neurilemmomas) (Fig 15); neurofibromas; fibrolipomatous hamartomas (also referred to as neural fibrolipomas, lipofibromas, encapsulated neuromas, or macrodystrophia lipomatosa); traumatic neuromas; and nerve sheath ganglia. Malignant peripheral neurogenic tumors are broadly classified under the umbrella term *malignant peripheral nerve sheath tumors*. Malignant peripheral nerve sheath tumors include malignant schwannomas, malignant triton tumors, malignant neurilemmomas, neurilemmosarcomas, neurofibrosarcomas, neurogenic sarcomas, and neurosarcomas (68). Mass lesions that may originate from surrounding soft tissues include ganglia and other cysts, enlarged lymph

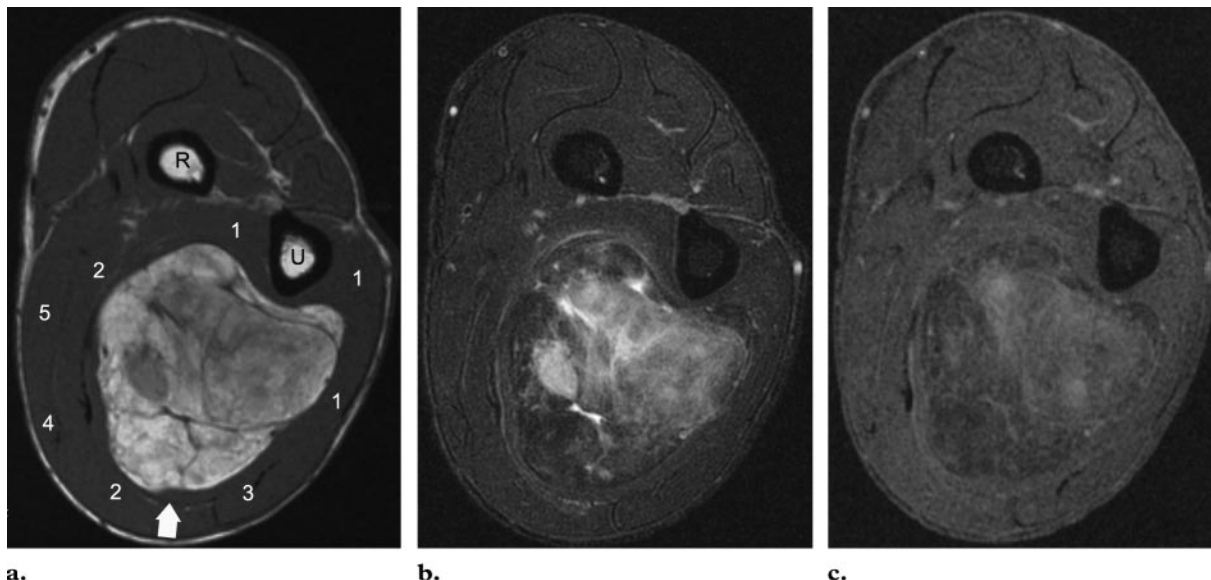


Figure 16. Histologically proved intramuscular lipoma in a 59-year-old man with swelling in the proximal part of the forearm and numbness in the ulnar aspect of the hand. **(a, b)** Axial T1-weighted SE MR image (460/14) **(a)** and T2-weighted fast SE MR image (2740/88; echo train length, 12) **(b)** at a proximal level in the forearm show an atypical lipoma within the flexor digitorum profundus muscle (1). The mass laterally displaces the flexor digitorum superficialis (2), flexor carpi ulnaris (3), palmaris longus (4), and flexor carpi radialis (5) muscles, as well as the ulnar nerve (arrow). R = radius, U = ulna. **(c)** Corresponding contrast-enhanced T1-weighted fat-suppressed SE MR image (420/14) shows inhomogeneous contrast enhancement of the lipoma.

nodes, lipomas (Fig 16), hemangiomas, and other benign or malignant soft-tissue tumors, as well as metastases from malignancies such as melanoma or breast cancer.

Summary

A broad variety of peripheral neuropathies may affect the median, radial, and ulnar nerves. Although a thorough clinical examination, combined with electrophysiologic studies, remains the cornerstone of the diagnostic work-up of peripheral neuropathies, in certain cases MR imaging may provide useful information with regard to the exact anatomic location of the lesion or may aid in narrowing the differential diagnosis. In patients with peripheral neuropathy, MR imaging may establish the origins of the condition and provide information crucial for management or surgical planning.

Acknowledgment: The authors thank Peter Roth for producing the schematics.

References

- Grant GA, Britz GW, Goodkin R, Jarvik JG, Maravilla K, Kliot M. The utility of magnetic resonance imaging in evaluating peripheral nerve disorders. *Muscle Nerve* 2002;25:314–331.
- Wein TH, Albers JW. Electrodiagnostic approach to the patient with suspected peripheral polyneuropathy. *Neurol Clin* 2002;20:503–526.
- Beltran J, Rosenberg ZS. Diagnosis of compressive and entrapment neuropathies of the upper extremity: value of MR imaging. *AJR Am J Roentgenol* 1994;163:525–531.
- Spratt JD, Stanley AJ, Grainger AJ, Hide IG, Campbell RS. The role of diagnostic radiology in compressive and entrapment neuropathies. *Eur Radiol* 2002;12:2352–2364.
- Sallomi D, Janzen DL, Munk PL, Connell DG, Tirman PF. Muscle denervation patterns in upper limb nerve injuries: MR imaging findings and anatomic basis. *AJR Am J Roentgenol* 1998;171:779–784.
- Spinner RJ, Amadio PC. Compressive neuropathies of the upper extremity. *Clin Plast Surg* 2003; 30:155–173.
- Bendszus M, Wessig C, Solymosi L, Reiners K, Koltzenburg M. MRI of peripheral nerve degeneration and regeneration: correlation with electrophysiology and histology. *Exp Neurol* 2004;188: 171–177.
- Wessig C, Koltzenburg M, Reiners K, Solymosi L, Bendszus M. Muscle magnetic resonance imaging of denervation and reinnervation: correlation with electrophysiology and histology. *Exp Neurol* 2004; 185:254–261.

9. May DA, Disler DG, Jones EA, Balkissoon AA, Manaster BJ. Abnormal signal intensity in skeletal muscle at MR imaging: patterns, pearls, and pitfalls. *RadioGraphics* 2000;20(Spec Issue):S295-S315.
10. Fleckenstein JL, Watumull D, Conner KE, et al. Denervated human skeletal muscle: MR imaging evaluation. *Radiology* 1993;187:213-218.
11. West GA, Haynor DR, Goodkin R, et al. Magnetic resonance imaging signal changes in denervated muscles after peripheral nerve injury. *Neurosurgery* 1994;35:1077-1086.
12. Goodpaster BH, Stenger VA, Boada F, et al. Skeletal muscle lipid concentration quantified by magnetic resonance imaging. *Am J Clin Nutr* 2004;79:748-754.
13. De Jesus R, Dellon AL. Historic origin of the "Arcade of Struthers." *J Hand Surg [Am]* 2003;28:528-531.
14. Pecina M, Boric I, Anticevic D. Intraoperatively proven anomalous Struthers' ligament diagnosed by MRI. *Skeletal Radiol* 2002;31:532-535.
15. Sener E, Takka S, Cila E. Supracondylar process syndrome. *Arch Orthop Trauma Surg* 1998;117:418-419.
16. Straub G. Bilateral supracondylar process of the humeri with unilateral median nerve compression in an 8-year-old child: a case report [in German]. *Handchir Mikrochir Plast Chir* 1997;29:314-315.
17. Rehak DC. Pronator syndrome. *Clin Sports Med* 2001;20:531-540.
18. Maravilla KR, Bowen BC. Imaging of the peripheral nervous system: evaluation of peripheral neuropathy and plexopathy. *AJNR Am J Neuroradiol* 1998;19:1011-1023.
19. Rosenberg ZS, Beltran J, Cheung YY, Ro SY, Green SM, Lenzo SR. The elbow: MR features of nerve disorders. *Radiology* 1993;188:235-240.
20. Hill NA, Howard FM, Huffer BR. The incomplete anterior interosseous nerve syndrome. *J Hand Surg [Am]* 1985;10:4-16.
21. Grunert J, Beutel F. Anterior interosseous nerve syndrome [in German]. *Unfallchirurg* 1999;102:384-390.
22. Kaufman MA. Differential diagnosis and pitfalls in electrodiagnostic studies and special tests for diagnosing compressive neuropathies. *Orthop Clin North Am* 1996;27:245-252.
23. al-Qattan MM, Robertson GA. Pseudo-anterior interosseous nerve syndrome: a case report. *J Hand Surg [Am]* 1993;18:440-442.
24. Verhagen WI, Dalman JE. Bilateral anterior interosseous nerve syndrome. *Muscle Nerve* 1995;18:1352.
25. Seror P. Pinch deficit of the thumb-index finger due to a lesion of the anterior interosseous nerve: apropos of 17 cases [in French]. *Ann Chir Main Memb Super* 1997;16:118-123.
26. Pierre-Jerome C, Bekkelund SI, Mellgren SI, Torbergsen T. Quantitative magnetic resonance imaging and the electrophysiology of the carpal tunnel region in floor cleaners. *Scand J Work Environ Health* 1996;22:119-123.
27. Jarvik JG, Yuen E, Kliot M. Diagnosis of carpal tunnel syndrome: electrodiagnostic and MR imaging evaluation. *Neuroimaging Clin N Am* 2004;14:93-102.
28. Jarvik JG, Yuen E, Haynor DR, et al. MR nerve imaging in a prospective cohort of patients with suspected carpal tunnel syndrome. *Neurology* 2002;58:1597-1602.
29. Horch RE, Allmann KH, Laubenberg J, Langer M, Stark GB. Median nerve compression can be detected by magnetic resonance imaging of the carpal tunnel. *Neurosurgery* 1997;41:76-83.
30. Bordalo-Rodrigues M, Amin P, Rosenberg ZS. MR imaging of common entrapment neuropathies at the wrist. *Magn Reson Imaging Clin N Am* 2004;12:265-279.
31. Fleckenstein JL, Wolfe GI. MRI vs EMG: which has the upper hand in carpal tunnel syndrome? *Neurology* 2002;58:1583-1584.
32. Thomas SJ, Yakin DE, Parry BR, Lubahn JD. The anatomical relationship between the posterior interosseous nerve and the supinator muscle. *J Hand Surg [Am]* 2000;25:936-941.
33. Kalb K, Gruber P, Landsleitner B. Compression syndrome of the radial nerve in the area of the supinator groove: experiences with 110 patients [in German]. *Handchir Mikrochir Plast Chir* 1999;31:303-310.
34. Rinker B, Effron CR, Beasley RW. Proximal radial compression neuropathy. *Ann Plast Surg* 2004;52:174-183.
35. Konjengbam M, Elangbam J. Radial nerve in the radial tunnel: anatomic sites of entrapment neuropathy. *Clin Anat* 2004;17:21-25.
36. Chien AJ, Jamadar DA, Jacobson JA, Hayes CW, Louis DS. Sonography and MR imaging of posterior interosseous nerve syndrome with surgical correlation. *AJR Am J Roentgenol* 2003;181:219-221.
37. Fernandez AM, Tiku ML. Posterior interosseous nerve entrapment in rheumatoid arthritis. *Semin Arthritis Rheum* 1994;24:57-60.
38. Dickerman RD, Stevens QE, Cohen AJ, Jaikumar S. Radial tunnel syndrome in an elite power athlete: a case of direct compressive neuropathy. *J Peripher Nerv Syst* 2002;7:229-232.
39. Genc H, Leventoglu A, Guney F, Kuruoglu R. Posterior interosseous nerve syndrome caused by the use of a Canadian crutch. *Muscle Nerve* 2003;28:386-387.
40. Yanagisawa H, Okada K, Sashi R. Posterior interosseous nerve palsy caused by synovial chondromatosis of the elbow joint. *Clin Radiol* 2001;56:510-514.

41. Mileti J, Largacha M, O'Driscoll SW. Radial tunnel syndrome caused by ganglion cyst: treatment by arthroscopic cyst decompression. *Arthroscopy* 2004;20:39–44.
42. Kalb K, Gruber P, Landsleitner B. Non-traumatically-induced paralysis of the ramus profundus nervi radialis: aspects of a rare disease picture [in German]. *Handchir Mikrochir Plast Chir* 2000;32:26–32.
43. Smola C. About the problem of radial tunnel syndrome or “where does the tennis elbow end and where does the radial tunnel syndrome begin?” [in German]. *Handchir Mikrochir Plast Chir* 2004;36:241–245.
44. Capitani D, Beer S. Handlebar palsy—a compression syndrome of the deep terminal (motor) branch of the ulnar nerve in biking. *J Neurol* 2002;249:1441–1445.
45. Bordalo-Rodrigues M, Rosenberg ZS. MR imaging of entrapment neuropathies at the elbow. *Magn Reson Imaging Clin N Am* 2004;12:247–263.
46. Posner MA. Compressive neuropathies of the ulnar nerve at the elbow and wrist. *Instr Course Lect* 2000;49:305–317.
47. Gonzalez MH, Lotfi P, Bendre A, Mandelbroyt Y, Lieska N. The ulnar nerve at the elbow and its local branching: an anatomic study. *J Hand Surg [Br]* 2001;26:142–144.
48. Bozkurt MC, Tagil SM, Ozcakar L. Guyon canal [letter]. *J Neurosurg* 2004;100:168.
49. Kim DH, Han K, Tiel RL, Murovic JA, Kline DG. Surgical outcomes of 654 ulnar nerve lesions. *J Neurosurg* 2003;98:993–1004.
50. Bui-Mansfield LT, Williamson M, Wheeler DT, Johnstone F. Guyon's canal lipoma causing ulnar neuropathy. *AJR Am J Roentgenol* 2002;178:1458.
51. Ruocco MJ, Walsh JJ, Jackson JP. MR imaging of ulnar nerve entrapment secondary to an anomalous wrist muscle. *Skeletal Radiol* 1998;27:218–221.
52. Dumontier C, Apoil A, Meininger T, Monet J, Augereau B. Compression of the deep branch of the ulnar nerve as it exits the pisiform-unciform hiatus: report of an anomaly not yet described [in French]. *Ann Chir Main Memb Super* 1991;10:337–341.
53. Haferkamp H. Ulnar nerve compression in the area of the wrist [in German]. *Langenbecks Arch Chir Suppl Kongressbd* 1998;115:635–640.
54. Kitamura T, Oda Y, Matsuda S, Kubota H, Iwamoto Y. Nerve sheath ganglion of the ulnar nerve. *Arch Orthop Trauma Surg* 2000;120:108–109.
55. Kobayashi N, Koshino T, Nakazawa A, Saito T. Neuropathy of motor branch of median or ulnar nerve induced by midpalm ganglion. *J Hand Surg [Am]* 2001;26:474–477.
56. Matsunaga D, Uchiyama S, Nakagawa H, Toriumi H, Kamimura M, Miyasaka T. Lower ulnar nerve palsy related to fracture of the pisiform bone in patients with multiple injuries. *J Trauma* 2002;53:364–368.
57. Nakamichi K, Tachibana S. Ganglion-associated ulnar tunnel syndrome treated by ultrasonographically assisted aspiration and splinting. *J Hand Surg [Br]* 2003;28:177–178.
58. Mondelli M, Mandarinini A, Stumpo M. Good recovery after surgery in an extreme case of Guyon's canal syndrome. *Surg Neurol* 2000;53:190–192.
59. Brantigan CO, Roos DB. Etiology of neurogenic thoracic outlet syndrome. *Hand Clin* 2004;20:17–22.
60. Aagaard BD, Lazar DA, Lankerovich L, et al. High-resolution magnetic resonance imaging is a noninvasive method of observing injury and recovery in the peripheral nervous system. *Neurosurgery* 2003;53:199–204.
61. Bendszus M, Stoll G. Caught in the act: in vivo mapping of macrophage infiltration in nerve injury by magnetic resonance imaging. *J Neurosci* 2003;23:10892–10896.
62. Perry JR, Fung A, Poon P, Bayer N. Magnetic resonance imaging of nerve root inflammation in the Guillain-Barre syndrome. *Neuroradiology* 1994;36:139–140.
63. Sander HW, Latov N. Research criteria for defining patients with CIDP. *Neurology* 2003;60(8 suppl 3):S8–S15.
64. Eurelings M, Notermans NC, Franssen H, et al. MRI of the brachial plexus in polyneuropathy associated with monoclonal gammopathy. *Muscle Nerve* 2001;24:1312–1318.
65. Van Es HW, Van den Berg LH, Franssen H, et al. Magnetic resonance imaging of the brachial plexus in patients with multifocal motor neuropathy. *Neurology* 1997;48:1218–1224.
66. Duggins AJ, McLeod JG, Pollard JD, et al. Spinal root and plexus hypertrophy in chronic inflammatory demyelinating polyneuropathy. *Brain* 1999;122(pt 7):1383–1390.
67. Jonas D, Conrad B, Von Einsiedel HG, Bischoff C. Correlation between quantitative EMG and muscle MRI in patients with axonal neuropathy. *Muscle Nerve* 2000;23:1265–1269.
68. Murphey MD, Smith WS, Smith SE, Kransdorf MJ, Temple HT. From the archives of the AFIP. Imaging of musculoskeletal neurogenic tumors: radiologic-pathologic correlation. *RadioGraphics* 1999;19:1253–1280.

Peripheral Neuropathies of the Median, Radial, and Ulnar Nerves: MR Imaging Features

Gustav Andreisek, MD et al

RadioGraphics 2006; 26:1267–1287 • Published online 10.1148/rg.265055712 • Content Codes:  

Page 1268

A normal nerve on T1-weighted images appears as a smooth round or ovoid structure with an MR signal that is isointense to that in adjacent muscle. A rim of hyperintense signal often surrounds peripheral nerves. The T1-weighted sequence, when applied after the administration of an extracellular gadolinium-based contrast agent, can be useful for demonstrating the anatomic relationship of nerve fascicles to closely associated mass lesions (see the section “Mass Lesions” in this article).

Page 1269

STIR sequences are particularly sensitive in depicting muscle edema (5,7). Neurogenic muscle edema occurs in acute and subacute stages of denervation and results in prolongation of the T2 relaxation time at MR imaging with T2-weighted or STIR sequences as early as 24–48 hours after denervation.

Page 1269

Neuropathies caused by entrapment of the median nerve include the supracondylar process syndrome, pronator syndrome, anterior interosseous nerve syndrome, and carpal tunnel syndrome.

Page 1275

Posterior interosseous nerve syndrome is a neuropathy caused by entrapment or compression of the radial nerve.

Page 1278

The neuropathies produced by entrapment of the ulnar nerve include cubital tunnel syndrome and Guyon canal syndrome.